EPJ Web of Conferences will be set by the publisher
DOI: will be set by the publisher

Semi-microscopic description of the proton- and neutron-induced backbending phenomena in some deformed even-even rare earth nuclei

R. Budaca[1,a] and A. A. Raduta[1,2]

[1] *Horia Hulubei National Institute of Physics and Nuclear Engineering, RO-077125 Bucharest-Magurele, Romania*
[2] *Academy of Romanian Scientists, 54 Splaiul Independentei, RO-050094 Bucharest, Romania*

Abstract. A semi-microscopic model to study the double backbending phenomenon in some deformed even-even nuclei from the rare earth region is proposed. The backbending phenomena are described by mixing four rotational bands, defined by a set of angular momentum projected states with a specific single-particle factor, and a model Hamiltonian describing a set of paired particles moving in a deformed mean field and interacting with a phenomenological deformed core. Due to the specific construction, the wave function acquires a complex structure which allows a quantitative description of the yrast states in the region of the two backbendings.

1 Introduction

The intersection of the ground band with a quasiparticle band built upon one or few broken pairs from a high angular momentum orbital causes an anomalous behavior of the moment of inertia in the yrast band known as backbending. In the rare earth region the first broken pair is from the neutron intruder orbital $1i_{13/2}$. The backbending is a relatively widespread phenomenon within the rare earth region, but only very few nuclei exhibit a second anomaly in the moment of inertia which is regarded as being caused by a successive breaking of a $1h_{11/2}$ proton pair. Here we present a simple semi-microscopic model for the simultaneous description of the proton- and neutron-induced backbending phenomena which are the results of the mixing between the ground band and decoupled $2qp$ and $4qp$ bands.

2 The theoretical model

The particle-core system is studied using the Hamiltonian $H = H_c + H_{sp} + H_{pair} + H_{pc}$ [1]. The core Hamiltonian H_c is a harmonic quadrupole boson operator:

$$H_c = \omega_0^b \hat{N} + \omega_1^b \hat{N}^2, \text{ where } \hat{N} = \sum_{\mu} b_{2\mu}^{\dagger} b_{2\mu}, \tag{1}$$

[a] e-mail: rbudaca@theory.nipne.ro

described by a phenomenological quadrupole coherent state $\psi_c = e^{d\left(b^\dagger_{20}-b_{20}\right)}|0\rangle_b$ [2]. As for the single-particle Hamiltonian H_{sp}, this is a sum of two spherical shell model terms corresponding to intruder neutrons and protons. The alike nucleons interact among themselves also through a pairing force.

The particle-core interaction consists of two terms $H_{pc} = H_{qQ} + H_{J_f J_c}$ [3]:

$$\begin{aligned} H_{qQ} &= -A_C \sum_{i=\nu,\pi} \sum_{\mu,m_i m_i'} \langle n_i l_i j_i m_i | r^2 Y_{2\mu} | n_i l_i j_i m_i' \rangle c^\dagger_{n_i l_i j_i m_i} c_{n_i l_i j_i m_i'} \left[(-)^\mu b^\dagger_{2-\mu} + b_{2\mu} \right], \\ H_{J_f J_c} &= C \vec{J}_f \cdot \vec{J}_c, \quad \text{with} \quad \vec{J}_f = \vec{J}_n + \vec{J}_p. \end{aligned} \tag{2}$$

The mean field is defined by averaging $\tilde{H}(= H_{sp} + H_{qQ})$ with the coherent state for the boson operators. In the first order of perturbation, its energies are given by

$$\varepsilon_{nljm} = \varepsilon_{nlj} - 4dX_C(2n+3) C^{j\,2\,j}_{\frac{1}{2}0\frac{1}{2}} C^{j\,2\,j}_{m0m}, \text{ with } X_C = \frac{\sqrt{5}\hbar A_C}{8\sqrt{\pi} M\omega_0}. \tag{3}$$

The sum of the mean field term and the pairing interaction for alike nucleons is then treated within the BCS formalism. The results of the BCS calculation corresponding to the neutron and proton intruder orbitals completely determine the single-particle factor state of the restricted particle-core space of angular momentum projected states with $0qp$, $2qp$ and $4qp$ which is defined by:

$$\begin{aligned} \Psi^{(1)}_{JM} &= \mathcal{N}^{(1)}_J P^J_{M0} |nBCS\rangle_d |pBCS\rangle_d \psi_c, \\ \Psi^{(2)}_{JM;1}(j_n\nu) &= \mathcal{N}^{(2)}_{J1}(j_n\nu) P^J_{M1} \left[J_+ \alpha^\dagger_{j_n\nu} \alpha^\dagger_{j_n-\nu} |nBCS\rangle_d \right] |pBCS\rangle_d \psi_c, \\ \Psi^{(3)}_{JM;1}(j_p\pi) &= \mathcal{N}^{(3)}_{J1}(j_p\pi) P^J_{M1} |nBCS\rangle_d \left[J_+ \alpha^\dagger_{j_p\pi} \alpha^\dagger_{j_p-\pi} |pBCS\rangle_d \right] \psi_c, \\ \Psi^{(4)}_{JM;2}(j_n\nu; j_p\pi) &= \mathcal{N}^{(4)}_{J2}(j_n\nu; j_p\pi) P^J_{M2} \left[J_+ \alpha^\dagger_{j_n\nu} \alpha^\dagger_{j_n-\nu} |nBCS\rangle_d \right] \left[J_+ \alpha^\dagger_{j_p\pi} \alpha^\dagger_{j_p-\pi} |pBCS\rangle_d \right] \psi_c. \end{aligned} \tag{4}$$

When applied on a $K = 0$ pair of quasiparticles, the operator J_+ simulates the breaking of the corresponding pair which acquires a projection $K = 1$. The projection of the core coherent state is completely described within the Coherent State Model [2]. While for angular momentum projection of the many-body fermion states one used the procedure of Ref.[4] taking into account the fact that Pauli principle restrains the maximal angular momentum of a given configuration to

$$J^{max}_\tau = N^{\tau j}_{pair} \left(2j_\tau - 2N^{\tau j}_{pair} + 1 \right), \tag{5}$$

where $N^{\tau j}_{pair}$ pairs of τ particles occupy the states of angular momentum j_τ.

The set of projected states mentioned above is not orthogonal, but using the eigenvalues and the eigenvectors of the overlap matrix one can construct an orthogonal basis [5]. The lowest eigenvalues of the total Hamiltonian H in this orthogonal basis define the yrast band and the total wavefunction is then given as an expansion in the same basis.

The quadrupole transition probabilities represent a very good test for the total wavefunctions corresponding to the yrast states. Here we suppose that the total transition is due to the core component of the wavefunction, such that the $E2$ transition probabilities are calculated by truncating the transition operator to the boson part [6],

$$Q_{2\mu} = q_1 \alpha_{2\mu} + q_2 (\alpha\alpha)_{2\mu}, \tag{6}$$

where $\alpha_{2\mu} = \frac{1}{\sqrt{2}} \left[b^\dagger_{2\mu} + (-)^\mu b_{2-\mu} \right]$ denotes the quadrupole collective coordinate. The microscopic structure of the yrast states have however an indirect contribution through the single-particle factor state.

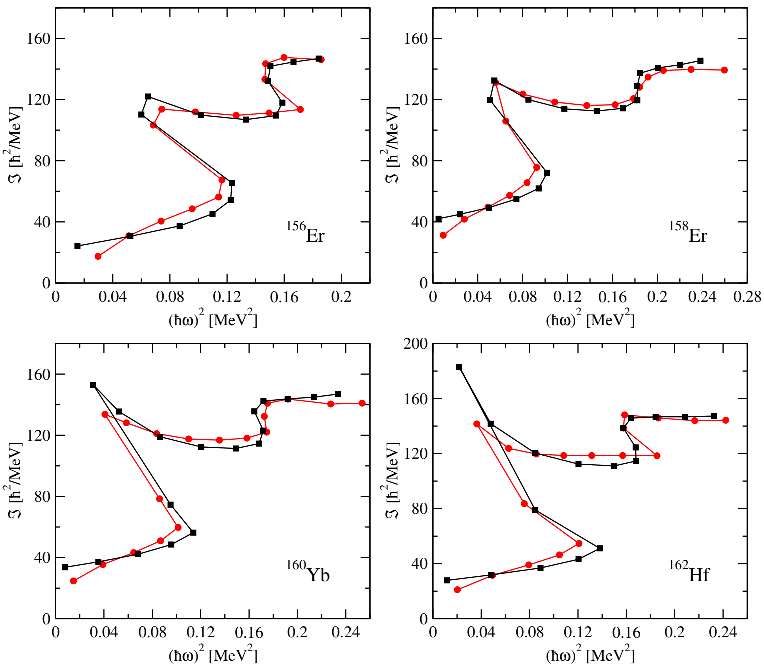

Figure 1. Backbending plots for ^{156}Er, ^{158}Er, ^{160}Yb and ^{162}Hf isotopes comparing theory (squares) with experiment (circles). Experimental data are taken from [9].

3 Numerical results

Four rare earth even-even nuclei which present the second anomaly in the observed moments of inertia are treated within the proposed model which involves seven parameters. Six of them, G_n, G_p, X_C, C, ω_0^b and ω_1^b are the structure coefficients defining the model Hamiltonian. The remaining parameter d defines the coherent state ψ_c and plays the role of the deformation parameter. Its numerical values happen to be in the range of values determined in [7, 8] for other isotopes of the nuclei treated here.

Using the calculated and measured energies of the yrast states one readily obtains the theoretical and experimental backbending curves. From Figure 1 it is obvious that the double zigzag shape is reproduced quite well for all four nuclei.

The transitions along the yrast band directly reflect the structural changes of the total wavefunction. In Figure 2 (left) one compares the theoretical predictions for $B(E2)$ with available experimental data [9] and the rigid rotor limit. From this figure one notes that at the first band crossing only one transition is sizably hindered while the second backbending leads to a less visible minimum of the transition probability in the corresponding band crossing region. This behavior is also found in the total gyromagnetic factor represented in Figure 2 (right) as function of total angular momentum J. Before the first band crossing it is almost constant and close to the rotational limit. Then it has a sudden fall down at the transition between the $0qp$ and $2qp$ states caused by the negative value of the neutron gyromagnetic factor coming from the decoupled neutron pair. After that, the rotation of the core starts to dominate, leading to an almost linear increase with J which only changes its slope at the second band crossing consistently with the slowness of the consequent breaking of the proton pair.

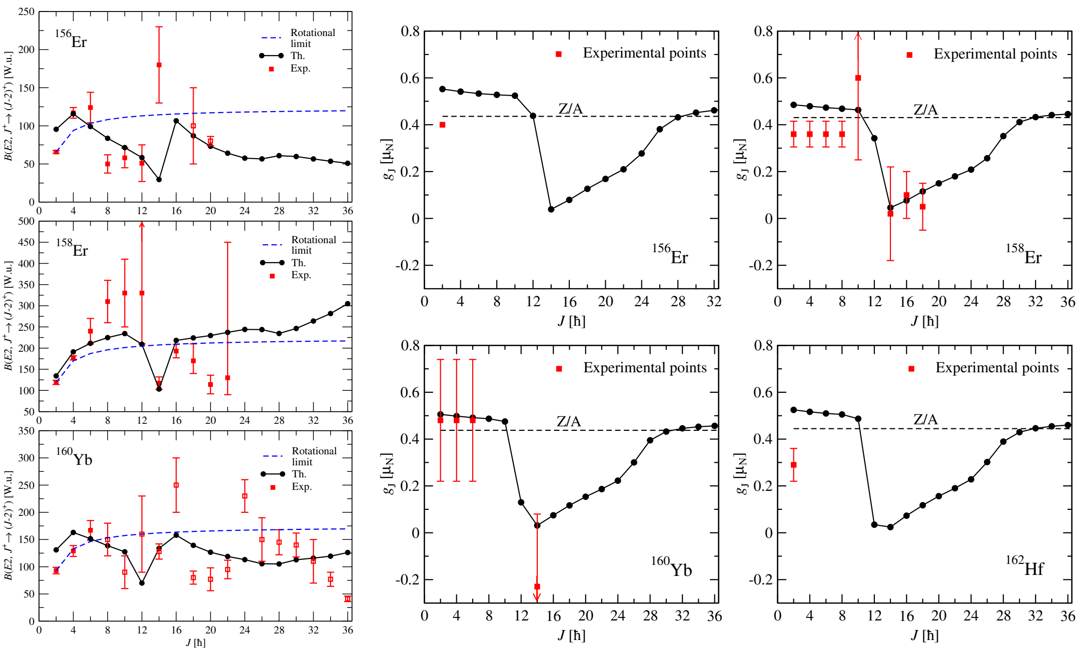

Figure 2. Electromagnetic properties of the treated nuclei along the yrast band. The theoretical results are compared with the available experimental data [9] for $E2$ probabilities (left) and gyromagnetic factors (right).

4 Conclusions

The present model provides a consistent explanation for the pair breaking process in connection with the rotational alignment of the angular momenta involved in the system. Based on the energy spectrum and the electromagnetic properties of the yrast states, one identified the major differences between the neutron- and the proton-induced backbendings. The theoretical results suggest that the proton pair breaking is a slower process than the neutron pair breaking.

The accuracy of description is reflected not only in the backbending plot but also by transition probabilities and gyromagnetic factors. As a final conclusion, one can say that the present formalism is able to quantitatively describe the double backbending phenomenon.

References

[1] R. Budaca and A. A. Raduta, J. Phys. G: Nucl. Part. Phys. **40**, 025109 (2013).

[2] A. A. Raduta, V. Ceausescu, A. Gheorghe and R. M. Dreizler, Nucl. Phys. A **381**, 253 (1982).

[3] A. A. Raduta and R. Budaca, Phys. Rev. C **84**, 044323 (2011); **87**, 029901(E) (2013).

[4] A. Kelemen and R. M. Dreizler, Z. Phys. A **278**, 269 (1976).

[5] A. A. Raduta, C. M. Raduta and A. Faessler, Phys. Rev. C **80**, 044327 (2009).

[6] A. A. Raduta, V. Ceausescu and A. Gheorghe, Nucl. Phys. A **311**, 118 (1978).

[7] A. A. Raduta, R. Budaca and A. Faessler, J. Phys. G: Nucl. Part. Phys. **37**, 085108 (2010).

[8] A. A. Raduta, R. Budaca and A. Faessler, Ann. Phys. (NY) **327**, 671 (2012).

[9] http://www.nndc.bnl.gov/ensdf/